Supporting Information: Polymorphism and solid solutions of trimethylammonium monocarboranes

*Jakob B. Grinderslev[1], Lasse N. Skov[1], Daniel R. Sørensen[1,2], Innokenty Kantor[2,3], Mads R. V. Jørgensen[1,2], Torben R. Jensen[1,]**

[1] Interdisciplinary Nanoscience Center (iNANO) and Department of Chemistry, Aarhus University, Langelandsgade 140, DK-8000 Aarhus C, Denmark

[2] MAX IV laboratory, Lund University, Fotongatan 2, SE 211 00 Lund, Sweden

[3] Department of Physics, The Technical University of Denmark, Fysikvej 3, DK-2880 Kgs. Lyngby, Denmark

* Corresponding author: trj@chem.au.dk, Tel: +45 8942 3894

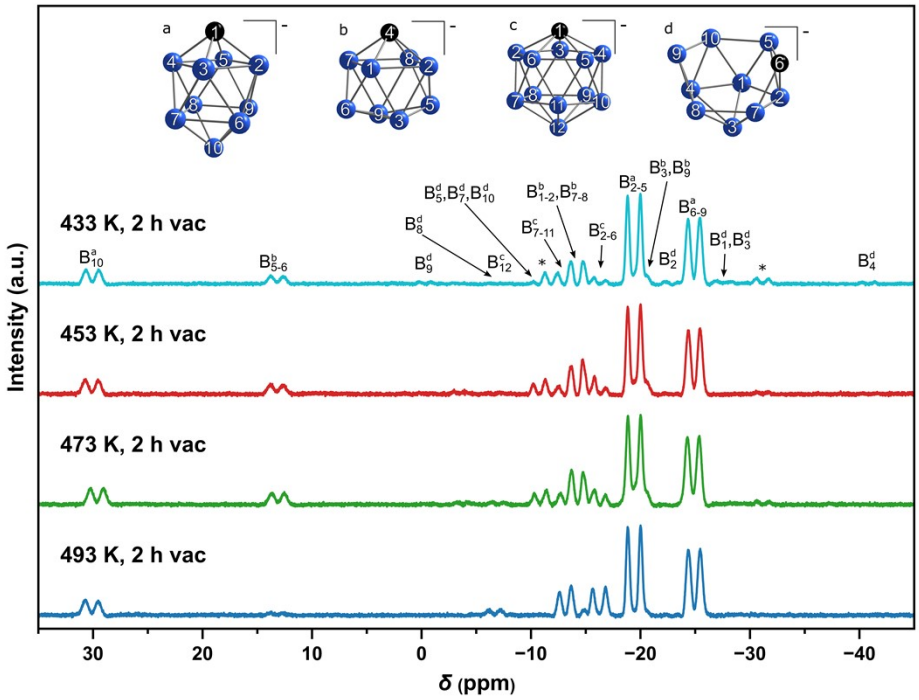

Figure S1. ^{11}B NMR spectra of $[NH(CH_3)_3][$*arachno*-6-$CH_2B_9H_{12}]$ (d) heated to either T = 433, 453, 473 or 493 K for 2 hours under dynamic vacuum, resulting in solid solutions of $[NH(CH_3)_3][(CB_8H_9)_x(CB_9H_{10})_y(CB_{11}H_{12})_z]$, containing the anions [*closo*-1-$CB_9H_{10}]^-$, [*closo*-4-$CB_8H_9]^-$ and [*closo*-1-$CB_{11}H_{12}]^-$, denoted a, b and c, respectively. '*' marks unknown B-species.

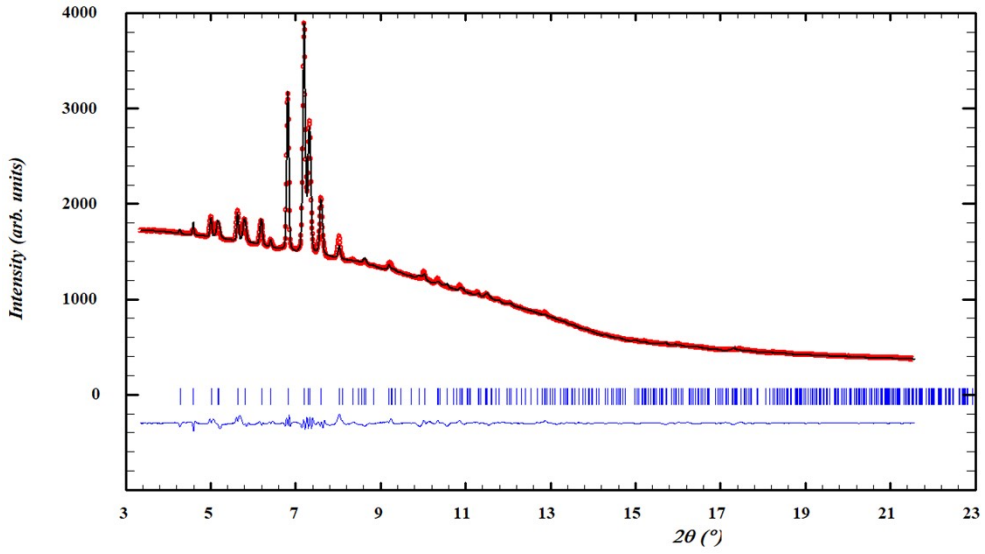

Figure S2. Rietveld refinement of the structural model of α-$[NH(CH_3)_3][CB_9H_{10}]$ from SR PXRD data measured at T = 273 K, λ = 0.6063 Å, showing experimental (red circles) and calculated (black line) PXRD patterns, and a difference plot below (blue line). Final discrepancy factors: R_p = 0.756 %, R_{wp} = 1.07 %, R_{exp} = 0.08 % (not corrected for background), R_p = 17.3 %, R_{wp} = 11.0

%, R_{exp} = 0.77 % (conventional Rietveld R-factors), R_{Bragg}(α-[$NH(CH_3)_3$][CB_9H_{10}]) = 9.80 % and global χ^2 = 203.

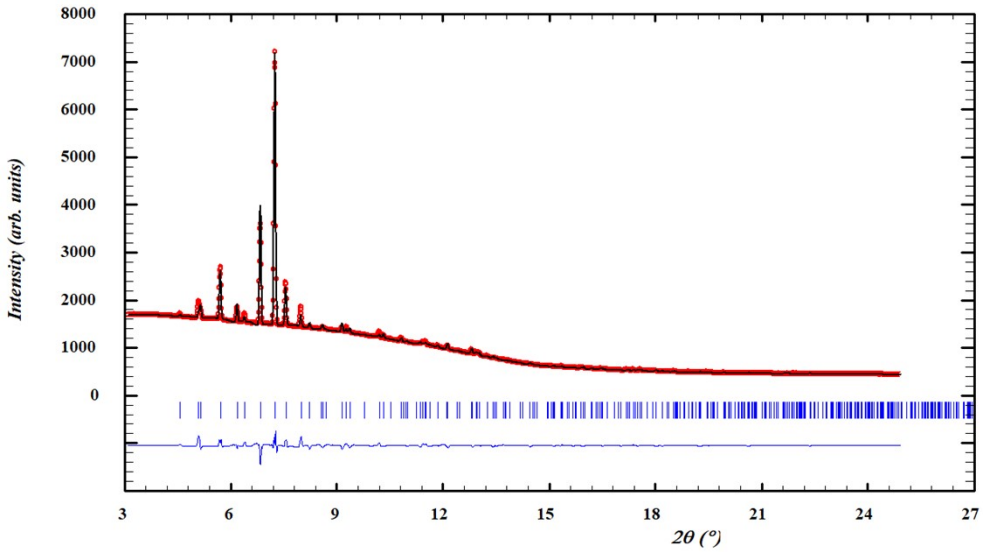

Figure S3. Rietveld refinement of the structural model of β-[$NH(CH_3)_3$][CB_9H_{10}] from SR PXRD data measured at T = 293 K, λ = 0.6063 Å, showing experimental (red circles) and calculated (black line) PXRD patterns, and a difference plot below (blue line). Final discrepancy factors: R_p = 1.03 %, R_{wp} = 1.63 %, R_{exp} = 0.08 % (not corrected for background), R_p = 23.7 %, R_{wp} = 13.6 %, R_{exp} = 0.66 % (conventional Rietveld R-factors), R_{Bragg}(β-[$NH(CH_3)_3$][CB_9H_{10}]) = 12.6 % and global χ^2 = 422.

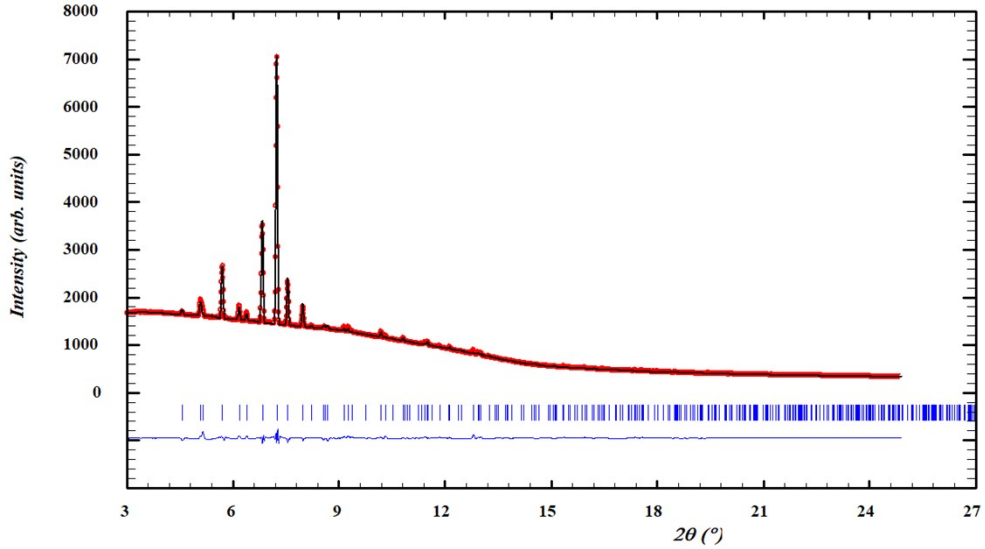

Figure S4. Rietveld refinement of the disordered structural model of β-[$NH(CH_3)_3$][CB_9H_{10}] from SR PXRD data measured at T = 293 K, λ = 0.6063 Å, showing experimental (red circles) and calculated (black line) PXRD patterns, and a difference plot below (blue line). Final discrepancy factors: R_p = 0.799 %, R_{wp} = 1.20 %, R_{exp} = 0.08 % (not corrected for background), R_p = 19.5 %,

R_{wp} = 9.97 %, R_{exp} = 0.67 % (conventional Rietveld R-factors), R_{Bragg}(β-[$NH(CH_3)_3$][CB_9H_{10}]) = 10.4 % and global χ^2 = 224.

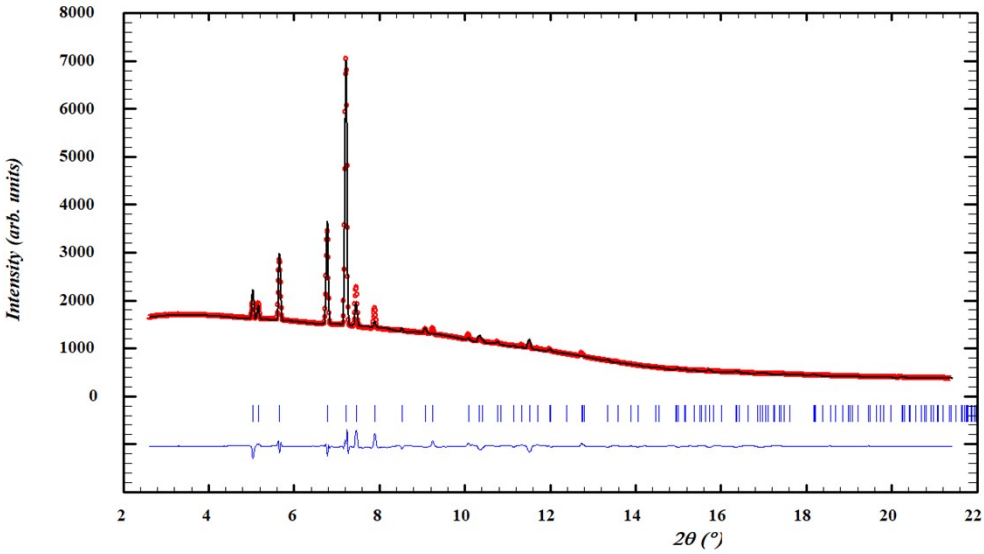

Figure S5. Rietveld refinement of the structural model of γ-[$NH(CH_3)_3$][CB_9H_{10}] from SR PXRD data measured at T = 340 K, λ = 0.6063 Å, showing experimental (red circles) and calculated (black line) PXRD patterns, and a difference plot below (blue line). Final discrepancy factors: R_p = 1.42 %, R_{wp} = 2.35 %, R_{exp} = 0.08 % (not corrected for background), R_p = 30.3 %, R_{wp} = 18.7 %, R_{exp} = 0.60 % (conventional Rietveld R-factors), R_{Bragg}(γ-[$NH(CH_3)_3$][CB_9H_{10}]) = 14.7 % and global χ^2 = 972.

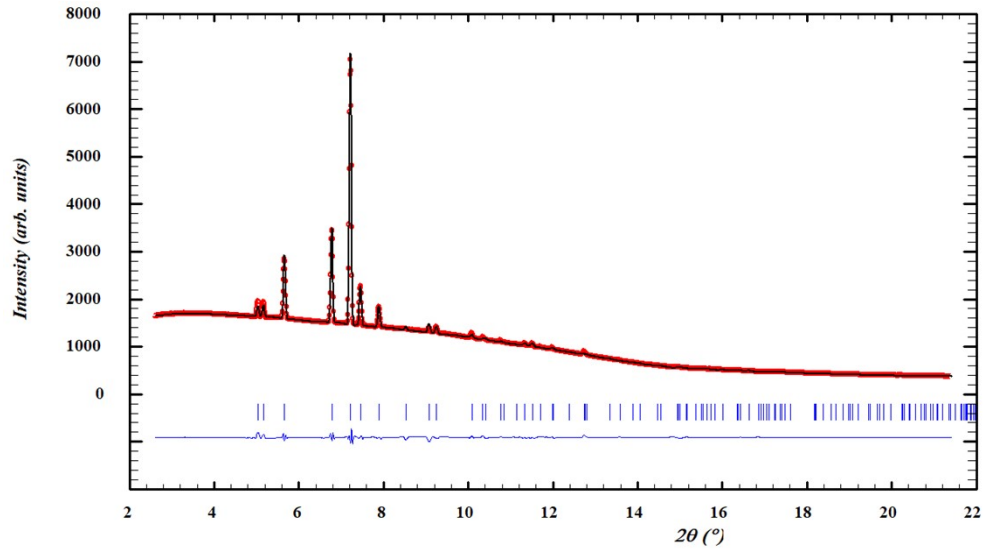

Figure S6. Rietveld refinement of the disordered structural model of γ-[$NH(CH_3)_3$][CB_9H_{10}] from SR PXRD data measured at T = 340 K, λ = 0.6063 Å, showing experimental (red circles) and calculated (black line) PXRD patterns, and a difference plot below (blue line). Final discrepancy

factors: R_p = 0.742 %, R_{wp} = 1.11 %, R_{exp} = 0.08 % (not corrected for background), R_p = 16.4 %, R_{wp} = 8.85 %, R_{exp} = 0.60 % (conventional Rietveld R-factors), R_{Bragg}(γ-[NH(CH$_3$)$_3$][CB$_9$H$_{10}$]) = 5.52 % and global χ^2 = 217.

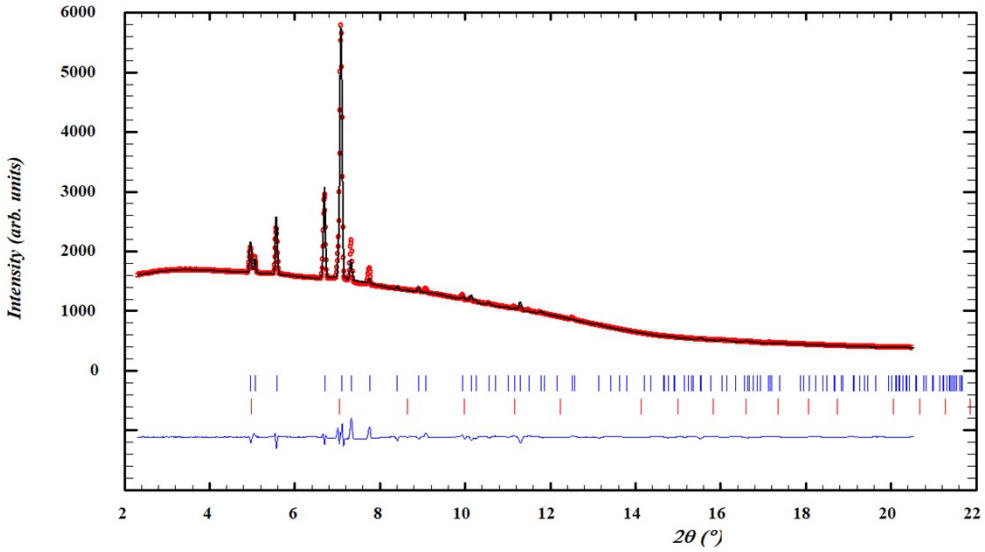

Figure S7. Rietveld refinement of the structural model of δ-[NH(CH$_3$)$_3$][CB$_9$H$_{10}$] from SR PXRD data measured at T = 500 K, λ = 0.6063 Å, showing experimental (red circles) and calculated (black line) PXRD patterns, and a difference plot below (blue line). Blue ticks: γ-[NH(CH$_3$)$_3$][CB$_9$H$_{10}$] (99.6 %), red ticks: δ-[NH(CH$_3$)$_3$][CB$_9$H$_{10}$] 0.4 %. Final discrepancy factors: R_p = 1.06 %, R_{wp} = 1.84 %, R_{exp} = 0.07 % (not corrected for background), R_p = 27.4 %, R_{wp} = 16.6 %, R_{exp} = 0.68 % (conventional Rietveld R-factors), R_{Bragg}(γ-[NH(CH$_3$)$_3$][CB$_9$H$_{10}$]) = 13.2 %, R_{Bragg}(δ-[NH(CH$_3$)$_3$][CB$_9$H$_{10}$]) = 6.40 % and global χ^2 = 606.

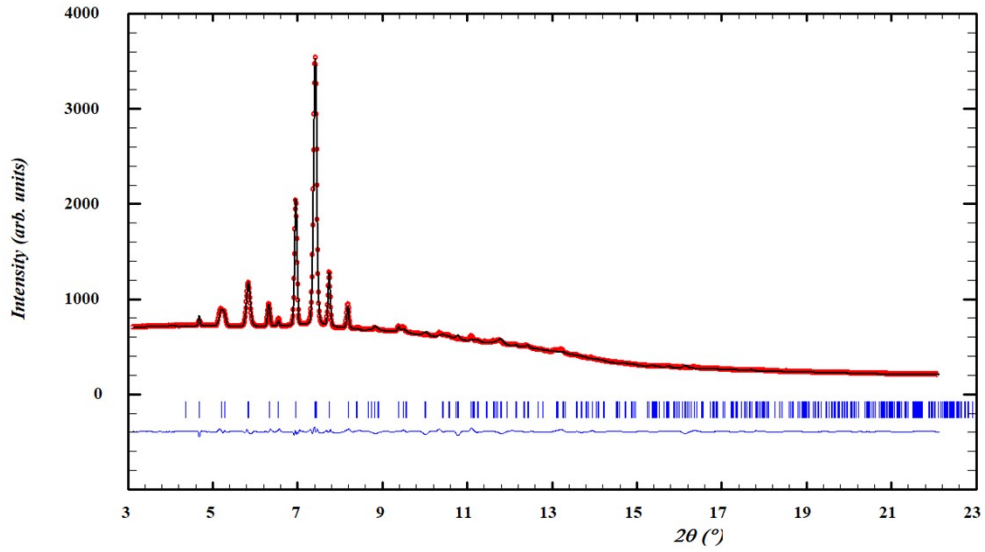

Figure S8. Rietveld refinement of the structural model of α-[NH(CH$_3$)$_3$][(CB$_8$H$_9$)$_{0.26}$(CB$_9$H$_{10}$)$_{0.66}$(CB$_{11}$H$_{12}$)$_{0.08}$] from SR PXRD data measured at T = 273 K, λ = 0.62028 Å, showing experimental (red circles) and calculated (black line) PXRD patterns, and

a difference plot below (blue line). Final discrepancy factors: R_p = 0.983 %, R_{wp} = 1.54 %, R_{exp} = 0.10 % (not corrected for background), R_p = 12.7 %, R_{wp} = 9.61 %, R_{exp} = 0.65 % (conventional Rietveld R-factors), R_{Bragg}(α-$[NH(CH_3)_3][(CB_8H_9)_{0.26}(CB_9H_{10})_{0.66}(CB_{11}H_{12})_{0.08}]$) = 7.16 % and global χ^2 = 218.

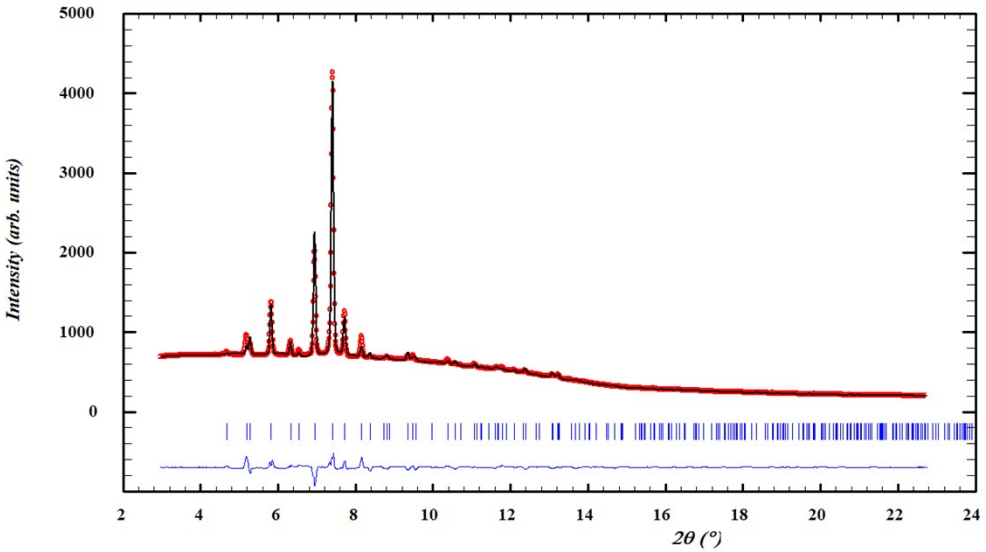

Figure S9. Rietveld refinement of the structural model of β-$[NH(CH_3)_3][(CB_8H_9)_{0.26}(CB_9H_{10})_{0.66}(CB_{11}H_{12})_{0.08}]$ from SR PXRD data measured at T = 293 K, λ = 0.62028 Å, showing experimental (red circles) and calculated (black line) PXRD patterns, and a difference plot below (blue line). Final discrepancy factors: R_p = 1.66 %, R_{wp} = 2.40 %, R_{exp} = 0.11 % (not corrected for background), R_p = 22.3 %, R_{wp} = 14.8 %, R_{exp} = 0.65 % (conventional Rietveld R-factors), R_{Bragg}(β-$[NH(CH_3)_3][(CB_8H_9)_{0.26}(CB_9H_{10})_{0.66}(CB_{11}H_{12})_{0.08}]$) = 12.4 % and global χ^2 = 519.

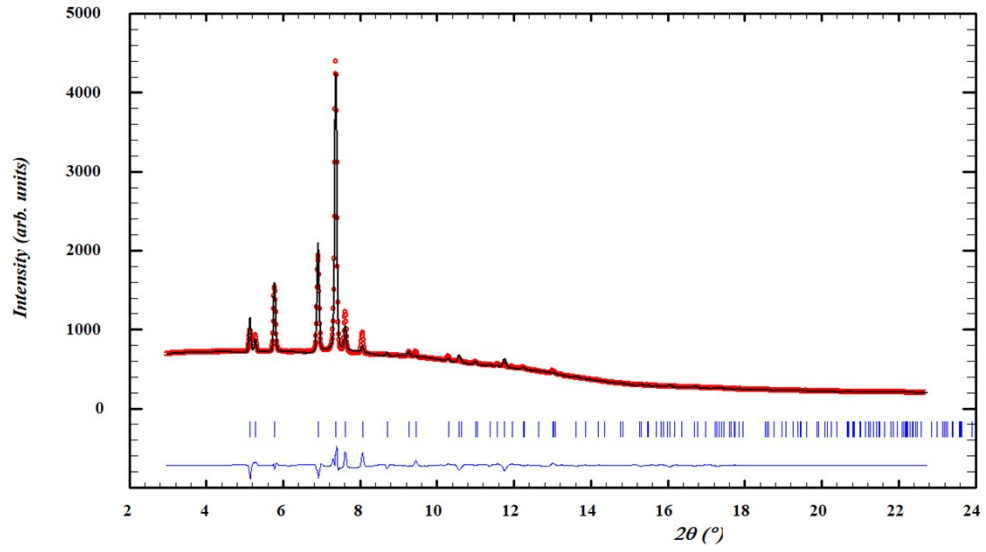

Figure S10. Rietveld refinement of the structural model of γ-$[NH(CH_3)_3][(CB_8H_9)_{0.26}(CB_9H_{10})_{0.66}(CB_{11}H_{12})_{0.08}]$ from SR PXRD data measured at T = 340 K, λ

= 0.62028 Å, showing experimental (red circles) and calculated (black line) PXRD patterns, and a difference plot below (blue line). Final discrepancy factors: R_p = 1.82 %, R_{wp} = 2.80 %, R_{exp} = 0.11 % (not corrected for background), R_p = 26.1 %, R_{wp} = 17.6 %, R_{exp} = 0.66 % (conventional Rietveld R-factors), R_{Bragg}(γ-$[NH(CH_3)_3][(CB_8H_9)_{0.26}(CB_9H_{10})_{0.66}(CB_{11}H_{12})_{0.08}]$) = 11.8 % and global χ^2 = 710.

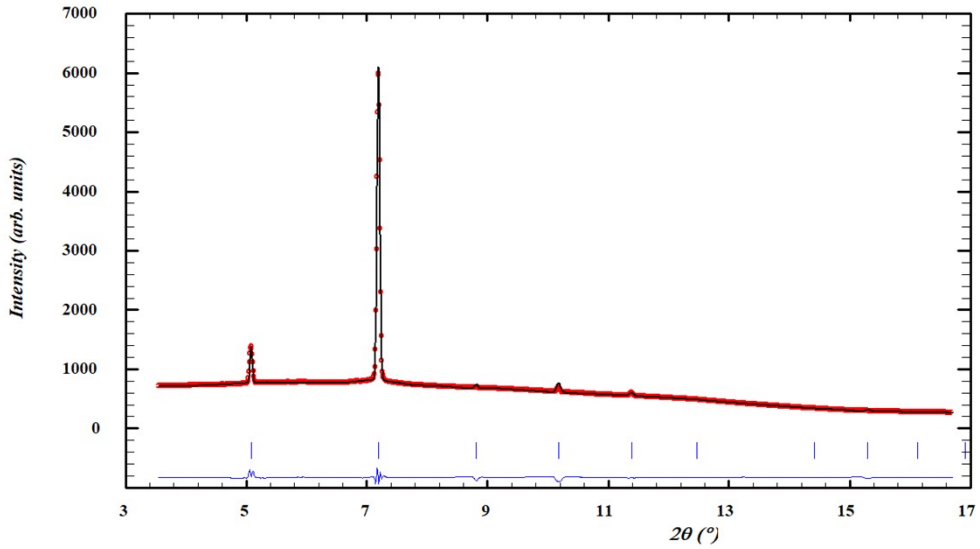

Figure S11. Rietveld refinement of the structural model of δ-$[NH(CH_3)_3][(CB_8H_9)_{0.26}(CB_9H_{10})_{0.66}(CB_{11}H_{12})_{0.08}]$ from SR PXRD data measured at T = 500 K, λ = 0.62028 Å, showing experimental (red circles) and calculated (black line) PXRD patterns, and a difference plot below (blue line). Final discrepancy factors: R_p = 0.931 %, R_{wp} = 1.70 %, R_{exp} = 0.10 % (not corrected for background), R_p = 16.2 %, R_{wp} = 9.61 %, R_{exp} = 0.54 % (conventional Rietveld R-factors), R_{Bragg}(δ-$[NH(CH_3)_3][(CB_8H_9)_{0.26}(CB_9H_{10})_{0.66}(CB_{11}H_{12})_{0.08}]$) = 1.11 % and global χ^2 = 315.

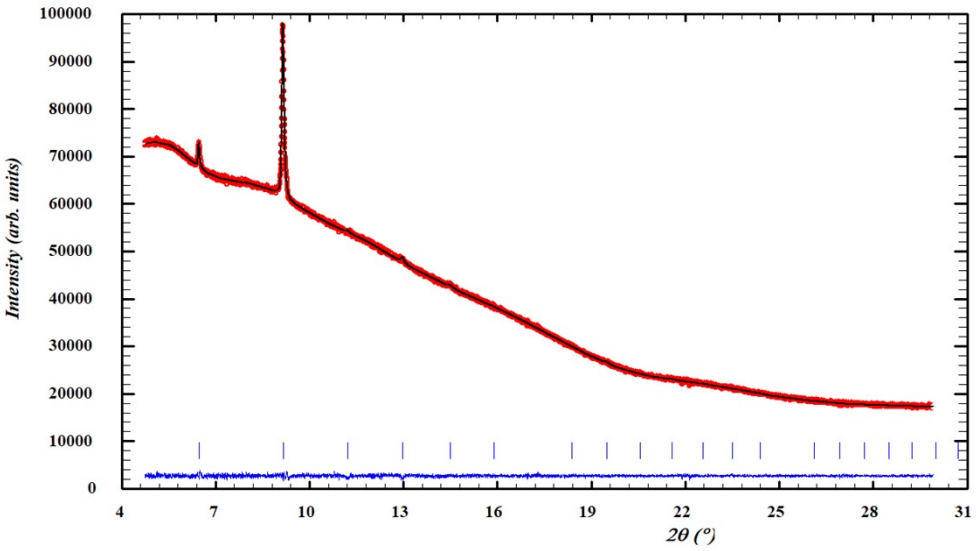

Figure S12. Rietveld refinement of the structural model of ε-$[NH(CH_3)_3][(CB_8H_9)_{0.26}(CB_9H_{10})_{0.66}(CB_{11}H_{12})_{0.08}]$ from SR PXRD data measured at T = 637 K, λ = 0.826366 Å, showing experimental (red circles) and calculated (black line) PXRD patterns, and a difference plot below (blue line). Final discrepancy factors: R_p = 0.418 %, R_{wp} = 0.540 %, R_{exp} = 0.52 % (not corrected for background), R_p = 67.4 %, R_{wp} = 15.4 %, R_{exp} = 14.89 % (conventional Rietveld R-factors), R_{Bragg}(ε-$[NH(CH_3)_3][(CB_8H_9)_{0.26}(CB_9H_{10})_{0.66}(CB_{11}H_{12})_{0.08}]$) = 2.81 % and global χ^2 = 1.13.

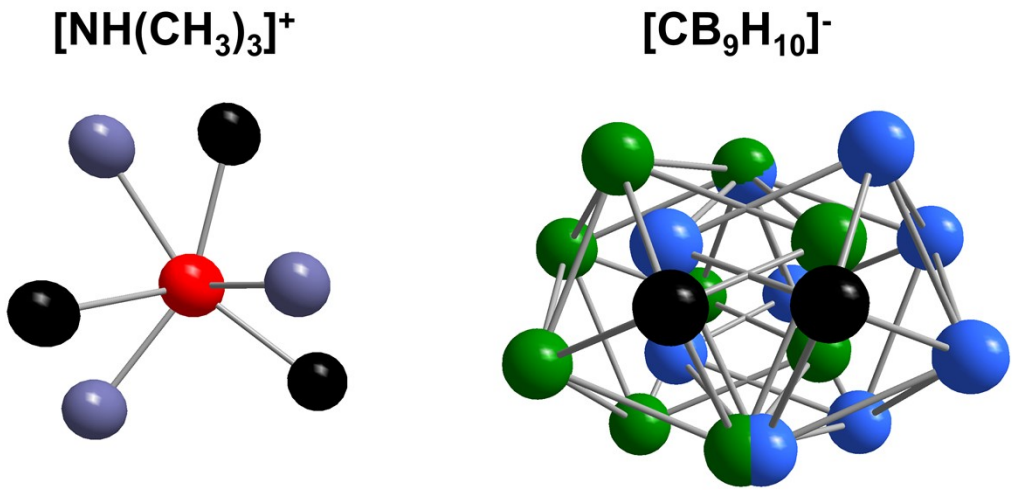

Figure S13. Disorder in β- and γ-$[NH(CH_3)_3][CB_9H_{10}]$ is observed for both the γ-$[NH(CH_3)_3]^+$ cation and the $[CB_9H_{10}]^-$, around a mirror-plane symmetry element with 50 % occupancy for each unit. Color scheme: B (blue/green), C (black/purple). N (red). H is omitted for clarity.

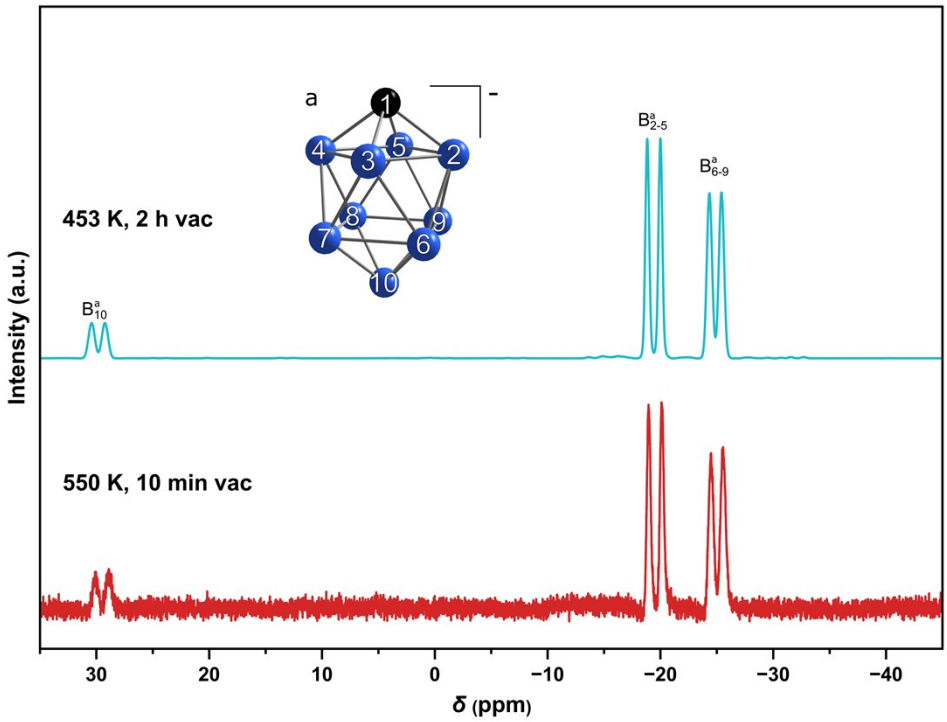

Figure S14. ^{11}B NMR spectra of $[NH(CH_3)_3][CB_9H_{10}]$ heated to T = 453 and 550 K for 2 hours under dynamic vacuum.